Research Square

Preprints are preliminary reports that have not undergone peer review.
They should not be considered conclusive, used to inform clinical practice,
or referenced by the media as validated information.

Polymer-Network 90°-Twisted Nematic Liquid Crystals with Spatially Partitioned Alignment for Linear-Polarization Rotation

Yi-Xuan Liu
National Central University
Pravinraj Selvaraj
National Central University
Chi-Tang Huang
National Central University
Chun-Ting Wu
National Central University
Wei-Chen Lee
National Central University
Ching-Cherng Sun
National Central University
Ko-Ting Cheng
chengkt@dop.ncu.edu.tw
National Central University

Article

Keywords: twisted nematic liquid crystal, polymer network, stabilization, linear polarization rotation

Posted Date: February 24th, 2026

DOI: https://doi.org/10.21203/rs.3.rs-8693652/v1

License: This work is licensed under a Creative Commons Attribution 4.0 International License.
Read Full License

Additional Declarations: No competing interests reported.

Abstract

We propose a spatial linear-polarization rotation scheme based on polymer-network 90° twisted nematic liquid crystals (PN-90°-TNLCs). By doping LC monomers into 90°-TNLCs and sequentially applying different electric voltages under simultaneous UV exposure, a PN-90°-TNLC cell with spatially partitioned LC alignment distributions is fabricated. This approach enables straightforward and stable generation of 1D and 2D spatial linear-polarization distributions. The polarization rotation angle of the output light, induced by the PN structures, remains stable after the electric stimuli are removed, demonstrating strong potential for optical information storage.

Introduction

The precise control of light polarization is an essential area of research with substantial applications in optical communication[1], sensing[2,3], and imaging[4,5]. Research has focused on developing linear polarization rotation devices based on liquid crystal (LC) optical elements, leveraging their intrinsic birefringence and electrically controllable properties. For instance, Guo *et al*. proposed an achromatic linear polarization rotator utilizing a hybrid splay–twisted LC cell with negative dielectric anisotropy[6]. This device enables continuous tuning of the LC configuration from a hybrid alignment to a 90° twisted nematic (TN) alignment under electric stimuli, thereby rotating the polarization direction of the output light by more than 90°. When Mauguin's condition is met, the device exhibits achromatic characteristics. To further enhance omnidirectional control of the output polarization direction, the same group subsequently proposed a linear polarization rotator based on a hybrid-alignment super-twisted LC cell composed of dual-frequency LCs[7]. This design achieves omnidirectional polarization rotation by switching an applied AC electric field between high- and low-frequency regimes using a single LC cell. However, this configuration requires a fixed β-angle, defined as the angle between the polarization direction of the incident light and the director of the LC layer close to the incident substrate, to be set at either 0° or 90°. Additionally, the large cell gap required to maintain achromaticity results in a wide operating voltage range, limiting practical applicability. To address this limitation, the same group proposed a linear polarization rotator using a hybrid splay–twisted LC cell with an enlarged twisted angle. The voltage required to rotate the polarization direction of the output light by 90° is significantly reduced, while extending the achievable output polarization rotation angle (PRA) to 135°, thereby meeting the requirements for optical communication applications[8].

Choi *et al.* explored a broadband, electrotunable linear polarization rotator incorporating interdigitated electrodes on one side of the substrates[9]. By applying an in-plane electric field generated by these electrodes, the LC configuration can be electrically switched between a homogeneous alignment and a 90° TN configuration. This design offers achromatic operation, a high degree of linear polarization (DoLP), and electrical tunability at relatively low operating voltages, making it a promising candidate for practical applications. Nonetheless, this approach presents challenges, including a longer response time than conventional TNLC devices and a restricted β-angle set to 0° or 90°. Additionally, dead zones arising

from the electric-field distribution of the interdigitated electrodes result in non-uniform behavior in the LC display[10].

In our previous research, we proposed achromatic, β-independent linear polarization rotators using tandem 90°-TNLC cells[11]. Through mathematical modeling, experimental validation, and simulations, we demonstrated that tandem TNLC systems effectively mitigate color dispersion and β-angle variations. However, satisfying Mauguin's condition requires the tandem TNLC cells to be sufficiently thick. Furthermore, applying an AC electric stimulus to the LC cell compromises the linear polarization retention of the output light transmitted through the tandem 90°-TNLC cells, thereby limiting their tunability in practical applications.

Recently, our team proposed an innovative approach employing a continuously tunable linear-polarization rotation mechanism based on a 90°-TNLC cell[12]. This advanced system ensures that the output-polarized light maintains a high DoLP, consistently exceeding 0.9. Mathematically, the DoLP is expressed as $\mathrm{DoLP} = (I_{\max} - I_{\min})/(I_{\max} + I_{\min})$, where I_{max} and I_{min} denote the intensities of the major and minor polarization components of the output polarized light, respectively[6,13]. This stable and continuous polarization rotation remains effective within a specific geometric parameter range characterized by dΔn/λ values between 1.27 and 1.7.

In this work, we expand the electrically tunable linear polarization rotation characteristics of 90°-TNLCs into a stabilized regime using polymer-network 90°-TNLCs (PN-90°-TNLCs). By doping LC monomers into the 90°-TNLCs and sequentially applying varying electric fields in conjunction with simultaneous UV exposure, we fabricate a PN-90°-TNLC cell featuring spatially partitioned LC alignment. This device produces a spatially varying distribution of output PRAs when linearly polarized light is incident at different locations. These results highlight the strong potential of this device for optical information storage applications with markedly enhanced storage capacity[14–16]. The detailed concept is presented in this paper.

Experimental section

This study utilizes an LC mixture consisting of 94.5 wt% nematic LC E7 (FUSOL-MATERIAL Co., Ltd), 5 wt% LC monomer RM257 (FUSOL-MATERIAL Co., Ltd), and 0.5 wt% photoinitiator DMPAP (Sigma-Aldrich, Merck). The ordinary refractive index (n_o) and extraordinary refractive index (n_e) of E7 at a wavelength of 633 nm are 1.51 and 1.73, respectively. For cell fabrication, two indium tin oxide-coated glass substrates were coated with polyvinyl alcohol (PVA) films to achieve a 90° TN alignment through orthogonal rubbing. The substrates were assembled with a uniform cell gap of approximately 5 μm, forming an empty cell that was filled with the above LC mixture. The polarized-light transmission characteristics of the LC cell were evaluated using a He-Ne laser (633 nm). The reference PRA is defined as the angle between the major axis of the output polarized light and the polarization direction of the incident linearly polarized light. To quantify the DoLP, a polarizing analyzer was placed between the LC

cell and a photodetector. The analyzer's transmission axis was adjusted to measure the maximum (I_{max}) and minimum (I_{min}) transmitted intensities.

Results and discussion

A. Simultaneous UV Exposure and Applied Electric Stimuli

In this study, we first aimed to ensure that the incorporation of LC monomers does not compromise the dynamic linear polarization rotation properties. We established a polymer network and stabilized the LC configuration within the 90°-TNLC cell by irradiating the monomer-doped LC mixture with 365 nm UV light (1 mW/cm²) while applying an external electric stimulus. Figure 1 shows the formation of the polymer network in the monomer-doped 90°-TNLC cell under simultaneous UV illumination and applied electric stimuli. The photoinitiator activates upon UV irradiation, generating reactive radicals that cleave the monomer double bonds, initiating polymerization. As polymer chains propagate, multifunctional monomers promote cross-linking, ultimately yielding a 3D polymer network[17–19]. Upon removal of the electric field, this polymer network effectively stabilizes the LC alignment, enabling sustained rotation of the transmitted light's linear polarization without further electrical stimulation. This approach improves understanding of LC dynamics and supports the development of photonic devices with tailored polarization properties.

B. Linear Polarization Rotation Properties Based on PN-90°-TNLCs

To evaluate the effect of monomer doping on the dynamic polarization rotation behavior of 90°-TNLCs, we compared the measured PRAs and DoLP for monomer-doped and undoped 90°-TNLCs, as shown in Fig. 2. The data reveal that the monomer-doped 90°-TNLC cell exhibits a continuous variation in PRA from 90° to 0° under applied electric stimuli, while maintaining a high DoLP (> 0.9). This result indicates that LC monomer doping does not compromise the dynamic polarization-rotation performance of the 90°-TNLC cell. To achieve stable output PRAs, we employed UV exposure (365 nm, 1 mW/cm²) to form a polymer network in a 90°-TNLC cell, effectively locking the LC structure after the applied electric stimulus was removed. When an external electric stimulus and UV illumination are simultaneously applied to the monomer-doped 90°-TNLC cell, phase separation occurs during UV curing. This phase separation facilitates monomer polymerization, leading to the formation of PN-90°-TNLCs. Upon removal of the electric field, the resulting polymer-network LC structures retain the linear polarization rotation of transmitted light without requiring additional electrical stimulation. As shown in Fig. 3, the measured PRAs and DoLP exhibit remarkable stability after UV illumination and the electric field are removed. These findings were obtained from separately prepared LC cells, confirming that the LC structure remains unchanged following polymer network establishment. The stabilized LC configurations consistently output PRAs while preserving a DoLP exceeding 0.9. These results underscore the effectiveness of polymer network formation in anchoring output PRAs in 90°-TNLC cells while

maintaining a high degree of linear polarization. Overall, combining UV curing with electrical stimulation improves the functional stability of LC devices for advanced optical applications.

C. Spatial Linear Polarization Distribution

Following confirmation of the polymer network's ability to stabilize the output PRAs, we systematically examined the performance of the PN-90°-TNLC cell, segmented into four regions. Each region was selectively exposed to 365 nm UV light (1 mW/cm²) under varying applied electric stimuli to develop a spatial linear polarization distribution in the output light. To maintain specific curing conditions, neighboring regions were shielded with black tape during UV illumination. This targeted curing process produced a spatially distinct polymer network, inducing position-dependent PRAs at the entry points of linearly polarized light into the PN-90°-TNLC cell. The PRAs and DoLP for each region were quantified after removing the applied electric field, as shown in Table 1. Upon exposing the PN-90°-TNLC cell at various locations, we observed a range of output PRAs, with DoLP values exceeding 0.9, indicating a high-quality spatial distribution of linearly polarized light. These findings highlight the effectiveness of localized UV curing in enhancing polarization management in LC systems, paving the way for advanced photonic applications that depend on sophisticated light manipulation.

To explore the spatial linear polarization rotation properties, we employed a polarizing analyzer to capture grayscale images of the output light as it propagated through the PN-90°-TNLC cell at different positions. Each of the four regions exhibited distinct PRAs, resulting in differential transmittance, as shown in Fig. 4**(b)**. A backlight unit with uniform intensity, powered by a tablet display designed in Microsoft PowerPoint 2021, illuminated the setup (model MYFQ2TA/Apple; RGB values: (255, 0, 0)). According to Malus' law, the linearly polarized beams transmitted through Regions #IV and #I displayed minimum and maximum intensities, respectively, as the angle between the incident polarized light and the analyzer approached 0°[20,21]. Adjusting the angle to 33° and 58° yielded maximum transmitted intensities through Regions #II and #III, respectively. At approximately 90°, Regions #IV and #I exhibited maximal and minimal transmission, respectively. Similarly, angles of 123° and 148° enabled light propagation in Regions #II and #III, respectively, at minimal intensity. These results demonstrate that the PN-90°-TNLC device successfully achieves a well-defined spatial distribution of linear polarization rotation. This capability underscores its strong potential for innovative applications in optical information-processing and data-storage systems. The precise manipulation of linear polarization presents new avenues for advancing photonic technologies, such as optical information and data storage.

Table 1
Relationship between applied voltages during UV curing and the resulting PRAs and DoLPs within the four partitioned regions of the 5-μm-thick PN-90°-TNLC cell. The *β*-angle was set at 90°.

	Applied Voltage (V_{rms})	Target PRA (°)	Measured PRA (°)	Measured DoLP
Region #I	5	0°	0°	0.944
Region #II	1.9	30°	33°	0.917
Region #III	1.6	60°	58°	0.931
Region #IV	1.35	90°	90°	0.941

D. Optical Information/Data Storage

The functionality of a linear polarization rotator-based PN-90°-TNLC cell can be used to achieve multilevel information/data storage in a single region (block). Recently, researchers have defined binary 0 and 1 using the transmittance of incoming light by utilizing LC birefringence. They have concurrently established two-bit binary values by manipulating the analyzer's rotation[14]. This approach also allows potential extension to octal elements by using transmittance to define binary 0 and 1. A conventional technique cannot overcome the restriction that only binary 0 and 1 can be written into a single layer at a single spot[15]. By establishing the linear PRA, the LC transmission can be calculated on the basis of the rotation of the analyzer. For example, octal values 0–7 can be encoded using output polarization directions of 0°, 13°, 26°, 39°, 52°, 65°, 78°, and 90°, with each value associated with a ± 6.5° tolerance range[16]. Within this tolerance, each polarization angle can be reliably identified as the corresponding octal digit. By employing four such regions, as shown in Fig. 4(b), a four-digit octal information storage system can be realized. Compared with a conventional four-bit binary system using the same number of regions (2^4 = 16 combinations), the proposed octal scheme provides a storage capacity of 8^4 (4,096), increasing the data storage capacity by a factor of 256, and substantially enhancing optical data density. For the four-digit octal information stored in the four-region PN-90°-TNLC, shown in Fig. 4(b), the output polarization directions of Regions #I to #IV are 0°, 33°, 58°, and 90°, corresponding to octal digits 0, 3, 4, and 7. The octal number 347 can be converted to 11100111 in binary and 231 in decimal. These findings demonstrate the potential applications in optical storage and encryption, including data storage and security devices, such as solid-state drives, optical discs, and hard disks.

Conclusion

We have successfully extended the electrically tunable linear polarization rotation properties of a 90°-TNLC configuration to stabilized linear polarization rotation using PN-90°-TNLCs. This work demonstrates a practical method for achieving designable, pixel-resolved linear polarization rotation using PN-90°-TNLCs. By subjecting a monomer-doped 90°-TNLC cell to stepwise UV exposure under varying electric fields, we fabricated a PN-90°-TNLC structure with pixel-like LC alignment. Once the

electric field was removed, the polymer network stabilized the LC configuration, resulting in distinct pixelized regions that exhibit position-dependent PRAs: Regions #I, #II, #III, and #IV correspond to PRAs of 0°, 33°, 58°, and 90°, respectively. This innovative approach allows the output PRA to vary with the incident position of linearly polarized light. As a result, spatial polarization distributions can be represented as grayscale intensity images using an analyzer, enabling optical information and data storage and other photonics applications.

Declarations

Disclosures

The authors declare no conflicts of interest.

Funding

National Science and Technology Council, Taiwan (113-2221-E-008-045-MY3, 114-2218-E-008-002).

Author Contribution

Y.-X. Liu, P. Selvaraj, and K.-T. Cheng wrote the main manuscript text. Y.-X. Liu, P. Selvaraj, C.-T. Huang, C.-T. Wu, W.-C. Lee, and K.-T. Cheng completed the methodology, validation, formal analysis, investigation, and data curation. Y.-X. Liu and P. Selvaraj prepared all the figures. C.-C. Sun played the role of funding acquisition. K.-T. Cheng played the role of supervision, project administration, and funding acquisition.

Data Availability

The data used in this work are not publicly available. However, they will be disclosed by the authors upon reasonable request.

References

1. Wu, C. et al. Highly polarization-deep-ultraviolet-sensitive β-Ga2O3 epitaxial films by disrupting rotational symmetry and encrypted solar-blind optical communication application. *J. Phys. Chem. Lett.* **15**, 3828–3834 (2024).
2. Zhang, Y. et al. Strain-enhanced polarization sensitivity in β-Ga2O3 photodetector. *Sci. China: Phys. Mech. Astron.* **67**, 247312 (2024).
3. Iglesias, W., Abbott, N. L., Mann, E. K. & Jákli, A. Improving liquid-crystal-based biosensing in aqueous phases. *ACS Appl. Mater. Interfaces*. **4**, 6884–6890 (2012).

4. Orlov, S. et al. Light engineering and silicon diffractive optics assisted nonparaxial terahertz imaging. *Laser Photonics Rev.* **18**, 2301197 (2024).
5. Baek, J., Kim, J., Seol, J. H. & Kim, M. All-dielectric polarization-sensitive metasurface for terahertz polarimetric imaging. *Sci. Rep.* **14**, 7544 (2024).
6. Guo, D. Y. et al. Electrotunable achromatic polarization rotator. *Optica* **8**, 364–371 (2021).
7. Chang, L. M. et al. Electrotunable 180° achromatic linear polarization rotator based on a dual-frequency liquid crystal. *Opt. Express*. **30**, 4886–4894 (2022).
8. Chen, J. Y., Chang, L. M. & Lin, T. H. Achromatic linear polarization rotator for optical communication wavelength range. *Opt. Express*. **33**, 36663–36671 (2025).
9. Choi, Y., Oh, S. W., Sohn, H. J. & Yoon, T. H. Broadband tunable polarization rotator based on the waveguiding effect of liquid crystals. *J. Phys. D: Appl. Phys.* **54**, 355108 (2021).
10. Choi, T. H., Choi, Y., Woo, J. H., Oh, S. W. & Yoon, T. H. Electro-optical characteristics of an in-plane-switching liquid crystal cell with zero rubbing angle: dependence on the electrode structure. *Opt. Express*. **24**, 15987–15996 (2016).
11. Chung, T. Y., Tsai, M. C., Liu, C. K., Li, J. H. & Cheng, K. T. Achromatic linear polarization rotators by tandem twisted nematic liquid crystal cells. *Sci. Rep.* **8**, 13691 (2018).
12. Cheng, K. T., Liu, Y. X., Huang, C. T. & Liu, C. K. Continuously electronically controlled linear polarization rotator. *US patent No US*. **11586058**, B1 (2023).
13. Liu, Y. X. et al. Advanced electrotunable linear polarization rotator with high degree of linear polarization using dye-doped 90°-twisted nematic liquid crystals. *Chin. J. Phys.* **95**, 205–211 (2025).
14. Xie, X. et al. Multichannel binary-image and holographic display based on planar liquid crystal devices. *Laser Photonics Rev.* **17**, 2300193 (2023).
15. Ivanov, S. S., Rangelov, A. A., Vitanov, N. V., Peters, T. & Halfmann, T. Highly efficient broadband conversion of light polarization by composite retarders. *J. Opt. Soc. Am. A*. **29**, 265–269 (2012).
16. Zhang, S. et al. Electrically switchable multicolored filter using plasmonic nanograting integrated with liquid crystal for optical storage and encryption. *Opt. Express*. **31**, 11940–11953 (2023).
17. Crivello, J. V. & Reichmanis, E. Photopolymer materials and processes for advanced technologies. *Chem. Mater.* **26**, 533–548 (2014).
18. Phillips, R. & Photopolymerization *J. Photochem.* **25**, 79–82 (1984).
19. March, N. H. & Tosi, M. P. *Polymers, Liquid Crystals, and Low-Dimensional Solids* (Springer, 2012).
20. Hecht, E. *Optics (4th edn)* (Addison Wesley, 2002).
21. Liu, C. K., Liao, M. C., Huang, C. T., Liao, S. H. & Cheng, K. T. Detection of polarization state of a polarized light using azimuthally symmetric dye-doped liquid crystals. *Dyes Pigm.* **204**, 110446 (2022).

Figures

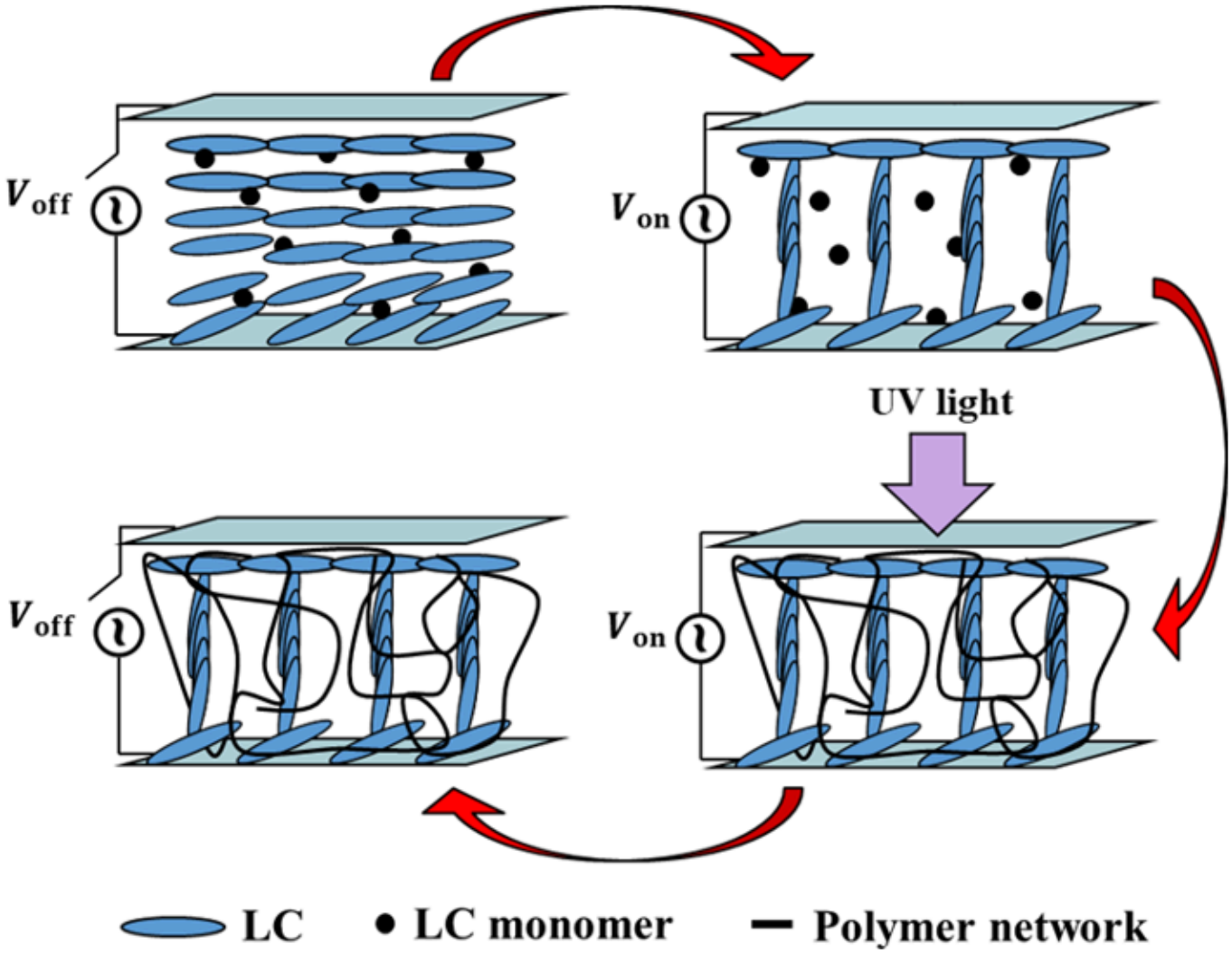


Figure 1

Schematic of a monomer-doped 90°-TNLC cell under simultaneous UV light exposure and applied electric stimuli.

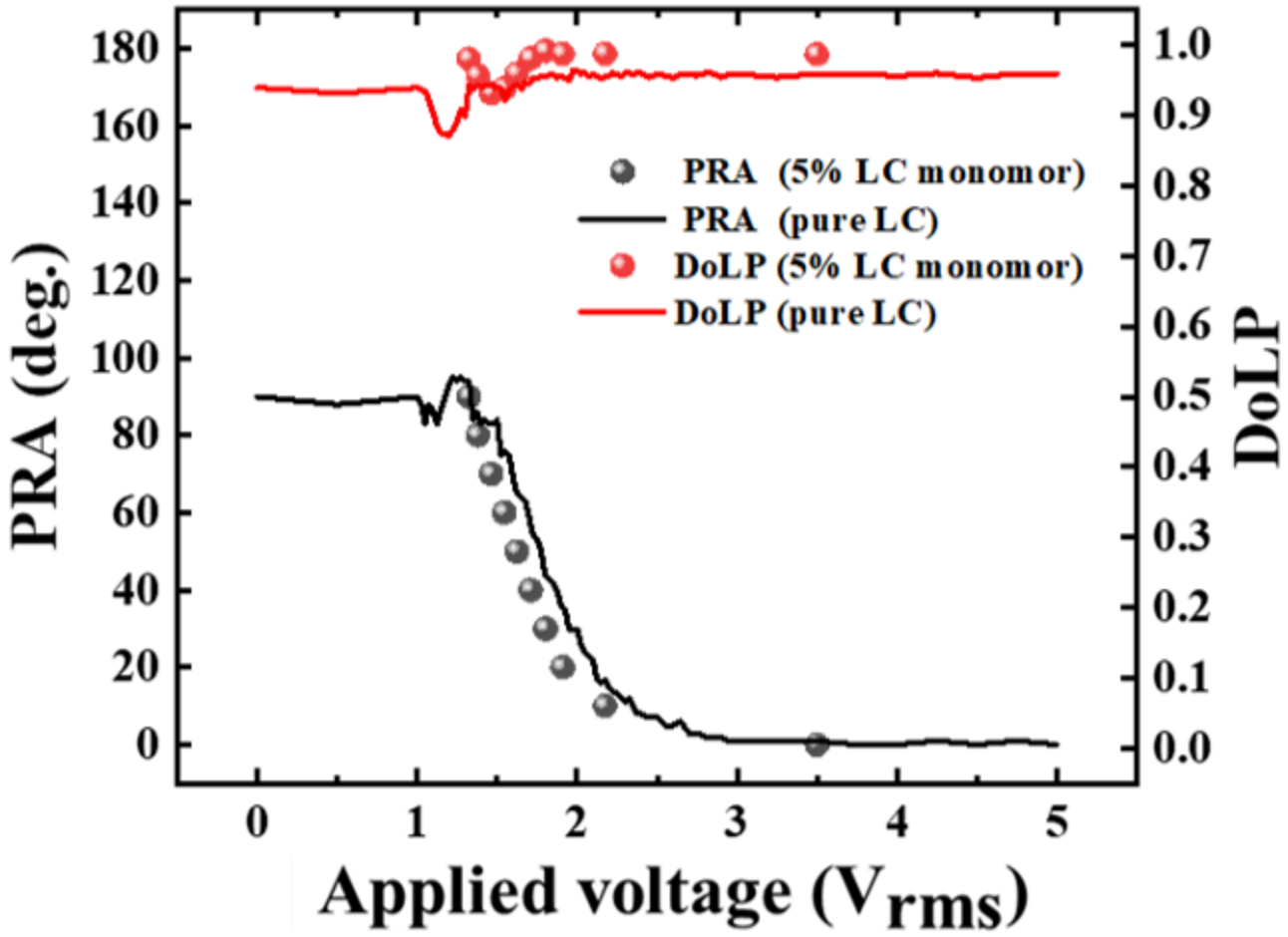


Figure 2

Experimental measurement of the PRA and DoLP for 5-μm-thick monomer-doped and undoped 90°-TNLC cells subjected to various applied electric stimuli, with the β-angle set at 90°.

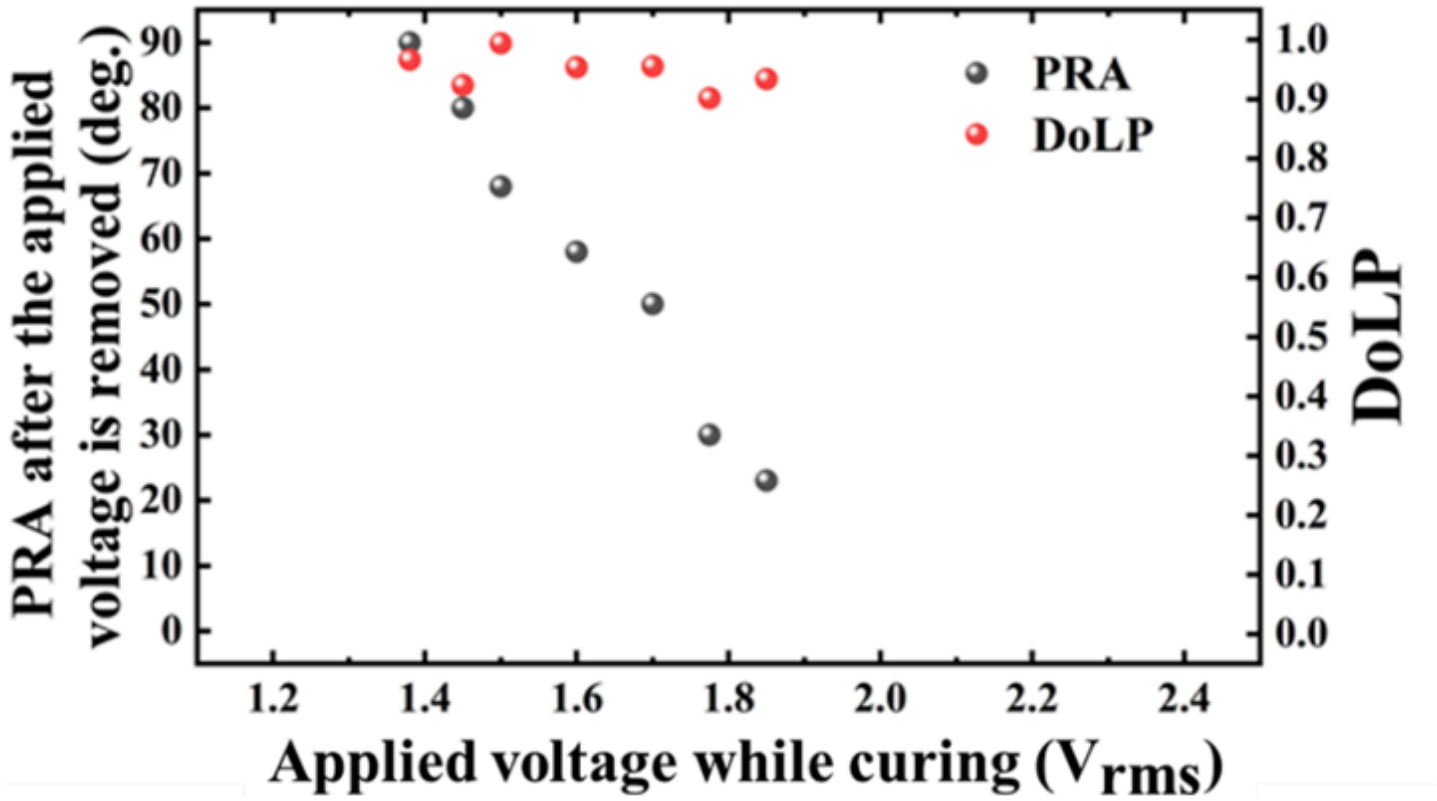


Figure 3

Evaluation of PRA and DoLP using PN-90°-TNLC cells. PRA and DoLP were assessed separately across different cell configurations and electrical stimuli, with the β-angle held constant at 90°.

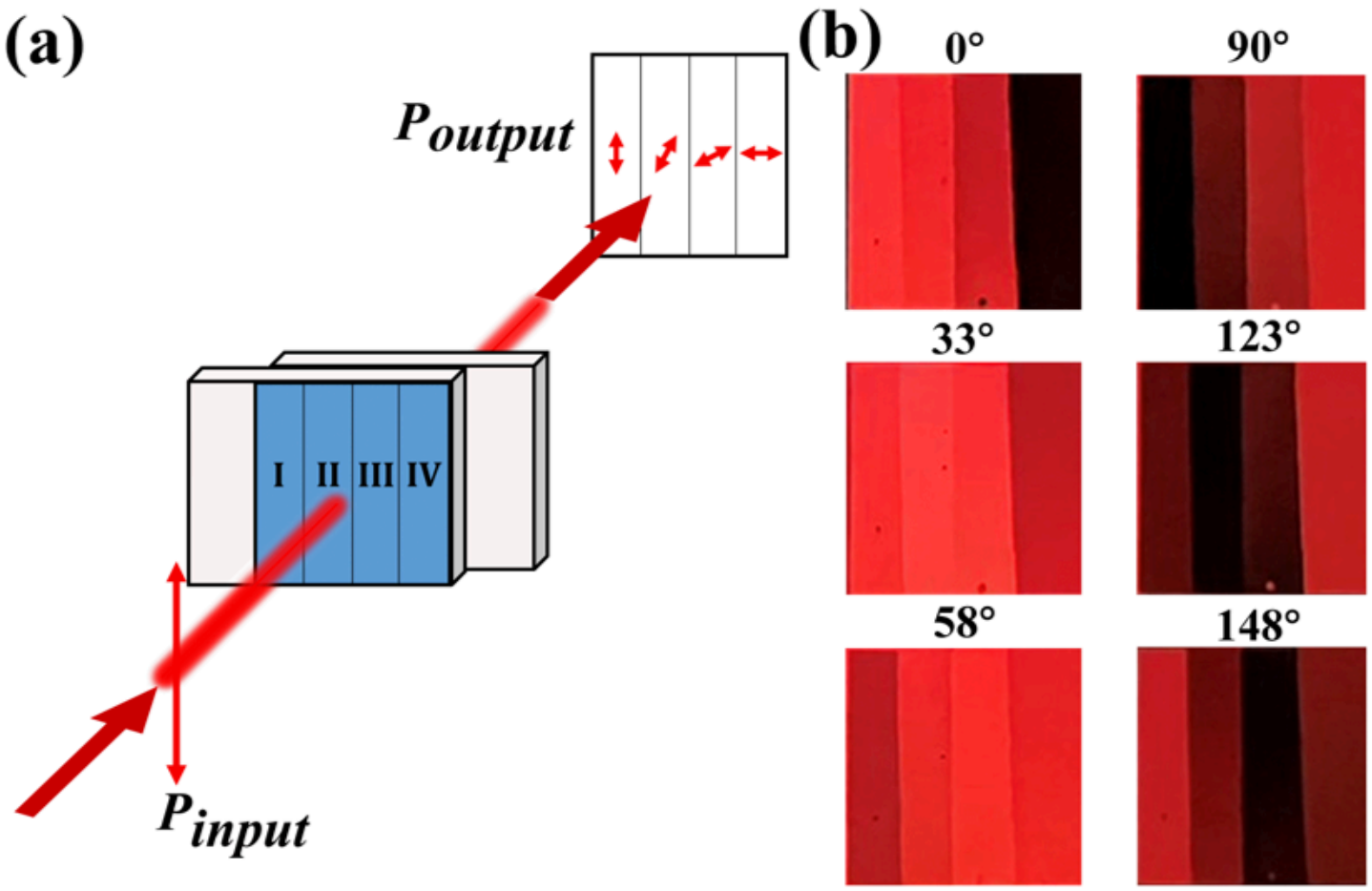


Figure 4

(a) Schematic of the PN-90°-TNLC cell subjected to partitioned curing, illustrating the linear polarization distribution at the output. (b) Experimental photographs of the PN-90°-TNLC cell, showcasing various angles between the polarizer and analyzer. The β-angle was set to 90°, whereas the remaining angles denote the orientations of the incident linearly polarized light (polarizer) and the analyzer.